Bioorg. Med. Chem. Lett. 40 (2021) 127952

Contents lists available at ScienceDirect

Bioorganic & Medicinal Chemistry Letters

journal homepage: www.elsevier.com/locate/bmcl

Discovery of β-carboline-(phenylsulfonyl)furoxan hybrids as potential anti-breast cancer agents

Xu Hu [a], Xiang Gao [a], Gang Gao [a], Yanbing Wang [b], Hao Cao [b,*], Dahong Li [a,*], Huiming Hua [a,*]

[a] Key Laboratory of Structure-Based Drug Design & Discovery, Ministry of Education, and School of Traditional Chinese Materia Medica, Shenyang Pharmaceutical University, 103 Wenhua Road, Shenyang 110016, PR China
[b] School of Life Science and Biopharmaceutics, Shenyang Pharmaceutical University, 103 Wenhua Road, Shenyang 110016, PR China

ARTICLE INFO

Keywords:
β-Carboline
NO donor
Breast cancer
Migration apoptosis

ABSTRACT

The cytotoxicity properties of the β-carboline alkaloids have been broadly investigated. However, the potential application of β-carbolines was hindered due to the moderate activity in cancer. In the present study, thirty β-carboline-(phenylsulfonyl)furoxan hybrids (**11a–j**, **12a–j** and **13a–j**) were designed and synthesized through esterification and amidation reaction strategy, and their inhibitory activities against the human breast cancer cell lines MCF-7 and MDA-MB-231 were evaluated by CCK-8 assay. Biological evaluation presented that the most promising amide derivative **13h**, substituted with *p*-methoxyphenyl group at position 1, generated high concentration of NO and evidently depressed the MCF-7 (IC_{50} = 0.89 μM) and MDA-MB-231 (IC_{50} = 0.62 μM) cells proliferation. Particularly, the wound healing and transwell assays demonstrated that **13h** significantly inhibited the migration and invasion of MDA-MB-231cells. Furthermore, the preliminary mechanisms studies indicated that **13h** induced G2/M phase arrest and apoptosis possibly causing by ROS accumulation and ROS-mediated DNA damage. Based on these considerations, **13h** may be a promising antimetastatic agent for breast cancer, which is noteworthy for further exploration.

Although substantial advances in treatment have been achieved, cancer remains the second leading cause of death globally in 2019, which outnumber the human immunodeficiency syndrome, malaria, and tuberculosis sum.[1] Strikingly, breast cancer, the most common malignant neoplasms affecting women, is the leading cause of cancer-associated deaths.[2,3] Currently, the treatment strategy for breast cancer mainly covers surgical mastectomy, hormone based therapies, radiation therapy, chemotherapy, and anti-angiogenic therapies based on tyrosine kinase receptors and hypoxia inducible factors (HIF) small molecule inhibitors and so on.[4] For estrogen receptor positive breast cancer, these therapies exert a better prognosis, however, which fail to produce prominent clinical benefits in the treatment of triple negative breast cancers (TNBC).[5,6] TNBC are short of human epidermal growth factor receptor 2 (HER2), progesterone receptor (PR), and estrogen receptor (ER) expression, possessing highly metastatic and aggressive with a worse prognosis.[7] Moreover, some targeted therapeutics are also barely satisfactory for TNBC.[8–11]

The alarming increase in cancer mortality has driven the search for new anti-tumor drugs, and one of the feasible ways to look for effective antineoplastic agents is still getting back to nature for answers.[12,13] At present, roughly 25% of drugs are arisen from natural resources, and the others are synthetic derivatives based on prototype compounds isolated from plants.[14] β-carboline alkaloids, possessing the common tricyclic pyrido-[3,4-b]indole ring, are mainly isolated from Zygophyllaceae,[15] Simaroubaceae,[16] Caryophyllaceae[17] and Rubiaceae.[18] Additionally, this class of alkaloids has been extensively researched due to their broad-spectrum of pharmacological activities, including anti-tumorigenic,[19] anti-Alzheimer's disease,[20] anti-Huntington's disease,[21] antidepressant,[22] anti-diabetic (inhibiting dual specificity tyrosine phosphorylation-regulated kinase 1A (DYRK1A)),[23] antimicrobial,[24] anti-inflammatory,[25] and antiplasmodial[26] effects and so on. Among them, the antitumor activity of β-carbolines has become a hot research topic. Accumulating evidences demonstrated that these alkaloids restrained cancer cell proliferation and induced apoptosis through diverse mechanisms, such as intercalating with DNA,[27] blocking angiogenesis,[28] depressing I-Kappa-B kinase (IKK),[29] topoisomerases I and II (Topo I and II),[30] mitogen activated protein kinase-activated protein kinase 2 (MK-2),[31] cyclin-dependent kinase (CDK),[32] polo-like kinase (PLK),[33] kinesin-like protein Eg5[34] and histone deacetylases (HDACs).[35] Recent studies indicated that harmine (Fig. 1) inhibited

* Corresponding authors.
E-mail addresses: caohao2008@163.com (H. Cao), lidahong0203@163.com (D. Li), huimhua@163.com (H. Hua).

https://doi.org/10.1016/j.bmcl.2021.127952
Received 29 January 2021; Received in revised form 26 February 2021; Accepted 7 March 2021
Available online 17 March 2021
0960-894X/

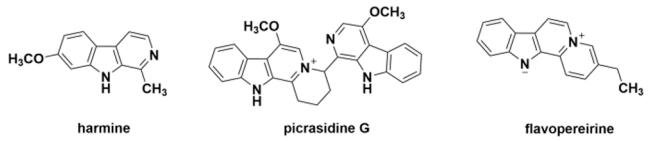

Fig. 1. Natural β-carboline alkaloids with anti-breast cancer properties.

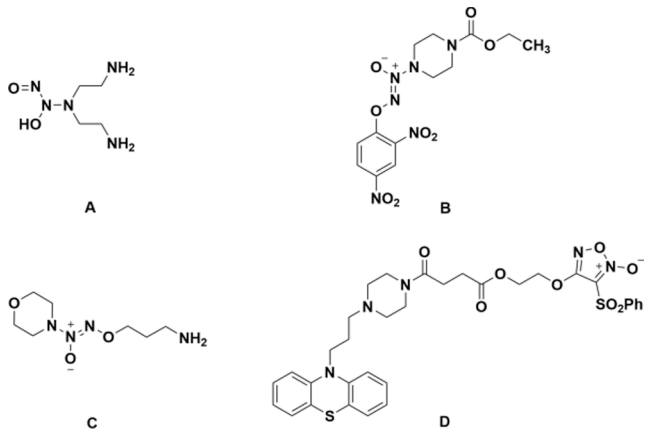

Fig. 2. NO donating derivatives with anti-breast cancer effects.

breast cancer resistance protein (BCRP) to decrease resistance to the anticancer drugs mitoxantrone and camptothecin in MDA-MB-231 cells.[36] Wink et al. showed that harmine suppressed telomerase activity of MCF-7 cells by down-regulating the expression of human telomerase reverse transcriptase (hTERT) mRNA, and inducing the accelerated senescence phenotype through the p53/p21 pathway.[37] Moreover, harmine restrained breast cancer cells growth and migration, induced apoptosis *in vitro* (MDA-MB-231 and MCF-7 cells) and *in vivo* (MCF-7 xenograft mice model), the underlying molecular mechanism identified that harmine exerted these properties through reducing the expression of transcriptional co-activator with PDZ-binding motif (TAZ), phosphorylation of extracellular regulated protein kinases (p-ERK), phosphorylation of v-Akt murine thymoma viral oncogene (p-Akt) and Bcl-2, and increasing Bax expression.[38] Picrasidine G (Fig. 1), a natural dimeric β-carboline, caused apoptosis and inhibited proliferation through aggrandizing chromatin condensation, sub-G1 population, cleavage of caspase 3 and poly(ADP-ribose) polymerase (PARP), suppressing the epidermal growth factor receptor (EGFR)-induced signal transducer and activator of transcription 3 (STAT3) phosphorylation and survivin transcription in the EGFR-overexpressed MDA-MB 468 cells.[39] In addition, Sheu et al. found that flavopereirine (Fig. 1) induced apoptosis and S phase cell cycle arrest via the Akt/p38/mitogen-activated protein kinases (MAPK)/ERK1/2 signaling pathway in MDA-MB-231 cells.[40]

Besides participating in a majority of physiological and pathophysiological processes, nitric oxide (NO) was found to be an effective anticancer candidate via different mechanisms, including ERK, Akt, mammalian target of rapamycin (mTOR), Ras, cyclin D1/retinoblastoma (Rb), nuclear factor kappa B (NF-κB) signaling pathways and so on.[41–43] Nevertheless, the role of NO is quite intricate in tumor biology, since it inhibits or promotes tumor proliferation mainly depending on concentration and cell sensitivity to NO.[44] It is worth mentioning that high concentration of NO released by NO donors not only induces tumor cells apoptosis through reducing the cell cycle proteins translation, but also sensitizes cells to radiation, immunotherapy, and chemotherapy *in vitro* and *in vivo*.[45–47] Engagingly, a recent study showed that NO-targeted therapy inhibited cancer stem cells and increased anti-hormonal therapy efficacy avoiding drug resistance in estrogen receptor-positive breast cancer cells.[48] Pervin et al. reported that DETA-NONOate (**A**) (Fig. 2), a long-acting NO donor, induced the mitochondrial apoptosis apoptosis in African American by enhancing Bax and reactive oxygen species (ROS) levels, activating caspase-3, and depolarizing mitochondrial membrane potential in TNBC.[49] Additionally, JS-K (**B**) (Fig. 2), a NO-releasing prodrug, induced autophagy by up-regulating microtubule light chain 3-II expression in breast cancer cells, while sparing normal mammary epithelial cells.[50] Subsequently, Huang et al. found that O^2-3-aminopropyl diazeniumdiolate (**C**) (Fig. 2) inhibited highly metastatic TNBC cells proliferation, and decreased adhesion, invasion and migration *in vitro*. Moreover, **C** also suppressed implanted TNBC growth and metastasis *in vivo* via blocking microvescile formation through NO-based epigenetic regulation of miR-203/RAB22A expression.[51] Considerable evidences suggest that NO donors may be potential benefits for the treatment of breast cancer.

Particularly interesting is the role of furoxans as NO donors in cancer cells, there was report that furoxan derivative (**D**) (Fig. 2) inhibited MCF-7 cells colony formation, and restrained MDA-MB-231 cells migration by down-regulating pNF-κB-p65 expression.[52] Our group has developed several (phenylsulfonyl)furoxan-based NO-donor derivatives possessing potent selective antitumor effects.[53–59] Given that both β-carboline and NO exert antiproliferative activity against breast cancer cells, we envisioned that novel furoxan/β-carboline hybrids could release high concentrations of NO, leading to superactive cytotoxicity against breast cancer cells. In the present study, a series of NO-releasing β-carboline derivatives (**11a–j**, **12a–j** and **13a–j**) were designed and synthesized by conjugating the carboxyl group of **5a–c** to phenylsulfonyl-substituted furoxan via different chemical linkers. Whereafter, their antiproliferative activity against MCF-7 and MDA-MB-231 cells, NO-releasing ability, cell cycle analysis, induction of apoptosis, comet assay, and the inhibitory effects of migration and invasion were evaluated.

The synthesis of target hybrids **11a–j**, **12a–j** and **13a–j** is illustrated in Scheme 1. The β-carboline intermediates **5a–c** were obtained by a four-step sequence. First, L-tryptophan **1** was treated with differently substituted aldehydes in the presence of sodium hydroxide solution or trifluoroacetic acid (TFA) and 1,2-dichloroethane (DCE) to offer **2a–c** by Pictet–Spengler reaction.[60] Then **3a–c** were prepared by esterification of **2a–c** through using $SOCl_2$. Meanwhile, **3a–c** were oxidized by $KMnO_4$ in anhydrous *N*,*N*-dimethylformamide (DMF) to afford **4a–c**. Finally, **4a–c** were hydrolyzed by sodium hydroxide to generate intermediates **5a–c**. Next, **9** was synthesized by a three-step strategy.[61] Briefly, benzenethiol **6** was reacted with chloroacetic acid to gain compound **7**. **7** was then oxidized by 30% H_2O_2 to give **8**. Diphenylsulfonylfuroxan **9** was synthesized from **8** accordingly with fuming HNO_3, which was next converted to diverse furoxan intermediates **10a–j** by reaction with various amino-substituted alcohol and diol. Finally, the treatment of β-carboline intermediates **5a–c** with furoxan derivatives **10a–f** in the presence of 4-dimethylaminopyridine (DMAP) and 1-(3-(dimethylamino)-propyl)-3-ethylcarbodiimide hydrochloride (EDCI) produced eighteen novel β-carboline/phenylsulfonylfuroxan derivatives **11a–f**, **12a–f** and **13a–f**. Simultaneously, twelve novel hybrids **11g–j**, **12g–j** and **13g–j** were synthesized by acylation of **5a–c** with **10g–j** under the condition of EDCI and 1-hydroxybenzotriazole (HOBT). The target compounds **11a–j**, **12a–j** and **13a–j** were purified by silica gel column chromatography, and all structures were identified by ^{1}H NMR, ^{13}C NMR, and high resolution mass spectrometry (HR-MS). (data in Supplementary Materials.)

To estimate the antineoplastic activity of the target derivatives, the inhibitory action on the proliferation of human mammary gland tumor cell line MCF-7 and TNBC cell line MDA-MB-231 was primarily tested by CCK-8 assay.[62] The IC_{50} values of all test compounds against two solid tumor cells are emerged in Table 1. The results displayed that most of the synthesized derivatives were remarkably more potent than the natural harmine. Eleven out of 30 hybrids even stronger than doxorubicin or **9**. The structure–activity relationships (SARs) analysis showed that **11a–j**, **12a–j** and **13a–j** with different linkers or a variety of 1-

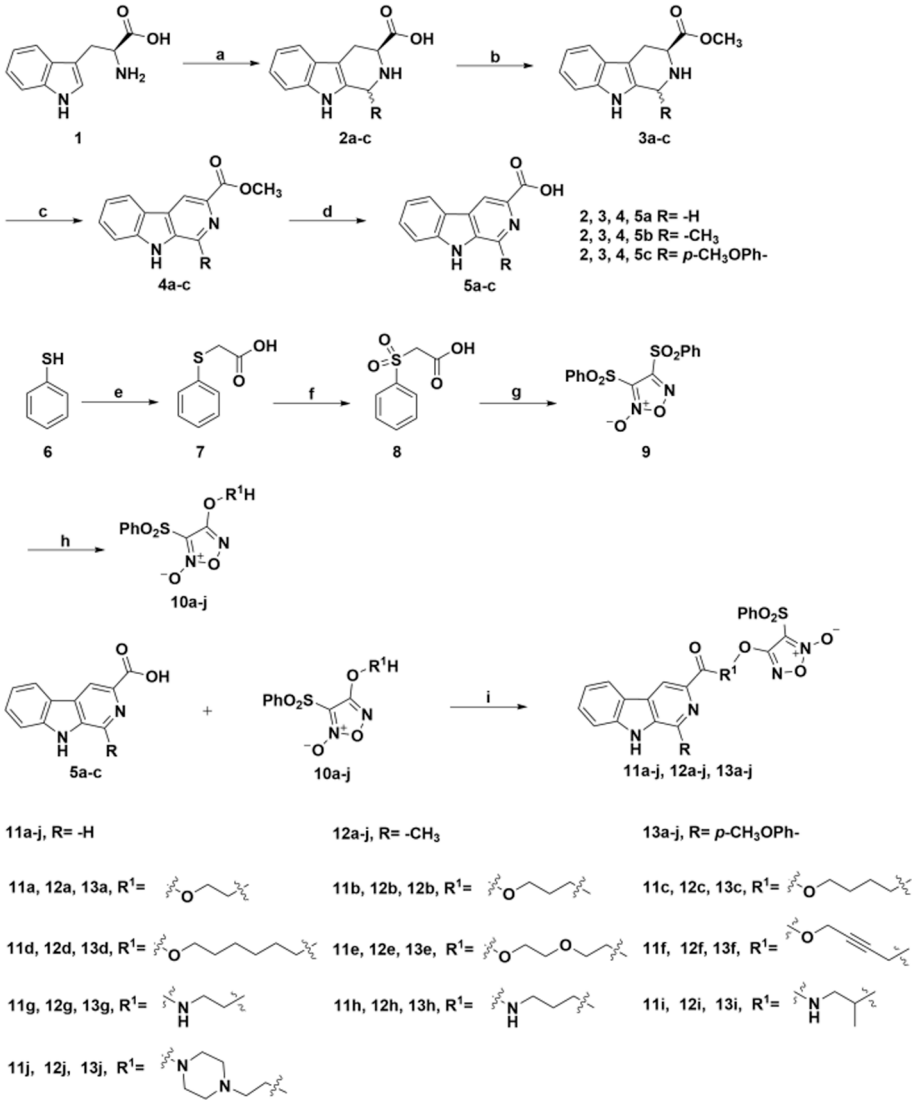

Scheme 1. Synthesis of compounds 11a–j, 12a–j and 13a–j. Reagents and conditions: (a) 0.4 N NaOH solution, 37% formaldehyde solution, 37 ℃, 3 d; or TFA, DCE, acetaldehyde/*p*-methoxybenzaldehyde, 110 ℃, 0.5 h; (b) $SOCl_2$, MeOH, 0 °C, 1 h, and then reflux, 6 h; (c) $KMnO_4$, anhydrous DMF, 0 °C, 1 h, and then rt, 24 h; (d) NaOH/MeOH, reflux, 6 h; (e) $ClCH_2COOH$, NaOH solution, reflux, 2 h; (f) 30% H_2O_2, AcOH, rt, 3 h; (g) Fuming HNO_3, 90 °C, 4 h; (h) Diol or alkanolamine, THF, NaH, 0 °C, 4 h; (i) 10a–f, EDCI, DMAP, anhydrous DCM, rt, 8–12 h; or 10g–j, HOBT, EDCI, anhydrous DCM, rt, 8–12 h.

Table 1
The antiproliferative activities of 11a–j, 12a–j and 13a–j against MCF-7 and MDA-MB-231 cells.

Compounds	IC_{50} (μM)[a]	
	MCF-7	MDA-MB-231
11a	11.47 ± 0.39	9.56 ± 0.43
11b	4.64 ± 0.28	7.96 ± 0.45
11c	9.57 ± 0.23	12.54 ± 0.68
11d	13.73 ± 0.70	8.87 ± 0.76
11e	19.04 ± 0.65	15.85 ± 0.52
11f	5.27 ± 0.40	5.89 ± 0.31
11g	7.53 ± 0.38	6.75 ± 0.47
11h	4.64 ± 0.44	7.50 ± 0.42
11i	6.94 ± 0.36	5.97 ± 0.27
11j	8.28 ± 0.47	6.83 ± 0.35
12a	4.58 ± 0.35	7.46 ± 0.37
12b	4.88 ± 0.19	2.24 ± 0.20
12c	4.28 ± 0.15	4.54 ± 0.22
12d	6.85 ± 0.30	5.75 ± 0.24
12e	5.89 ± 0.41	7.67 ± 0.52
12f	8.86 ± 0.48	6.91 ± 0.55
12g	4.96 ± 0.35	3.84 ± 0.16
12h	2.97 ± 0.14	1.62 ± 0.10
12i	3.80 ± 0.17	2.20 ± 0.15
12j	3.29 ± 0.27	3.47 ± 0.19
13a	4.80 ± 0.16	3.59 ± 0.29
13b	3.49 ± 0.16	2.86 ± 0.22
13c	2.92 ± 0.27	4.26 ± 0.29
13d	5.36 ± 0.32	2.98 ± 0.44
13e	3.92 ± 0.21	2.53 ± 0.26
13f	2.35 ± 0.27	1.16 ± 0.08
13g	1.45 ± 0.12	0.87 ± 0.05
13h	0.89 ± 0.05	0.62 ± 0.05
13i	1.56 ± 0.10	2.27 ± 0.16
13j	1.33 ± 0.11	0.92 ± 0.04
5a	> 30	> 30
5b	19.24 ± 0.67	22.64 ± 0.86
5c	14.30 ± 0.32	12.63 ± 0.28
9	3.92 ± 0.10	4.84 ± 0.22
harmine	16.94 ± 0.47	21.91 ± 1.25
doxorubicin	3.09 ± 0.16	2.86 ± 0.18

[a] IC_{50}: Half inhibitory concentrations were measured by the CCK-8 assay, cells were treated with indicated compounds for 72 h, and the values are expressed as averages ± standard deviations of three independent experiments.

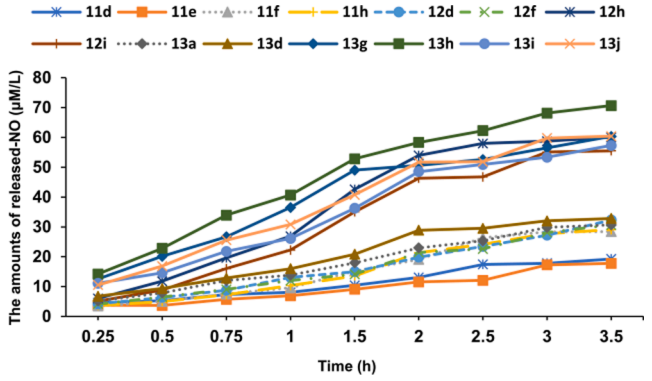

Fig. 3. NO-releasing ability of several selected target compounds. The values are expressed as averages of three independent experiments.

substituted β-carbolines indicated discrepant antiproliferative activity against breast cancer cells. For instance, the antitumor activity of β-carbolines derivatives (**13a–j**) substituted with *p*-methoxyphenyl group at position 1 was significantly stronger than that of analogues substituted with methyl (**12a–j**) or H (**11a–j**) at position 1, which reflected that the steric hindrance and electric effect of substituted groups were of great importance in the biological activities. Furthermore, the compounds (**11g–j**, **12g–j** and **13g–j**) linked with alkanolamine presented more potent inhibitory activity than the compounds (**11a–f**, **12a–f** and **13a–f**) linked with diol, which might be due to the fact that the ester-linked hybrids were usually easily metabolized into acids and alcohols in the body to cause weakened activity. As a matter of fact, the ester derivatives (**11a**, **11c**, **11d** and **11e**) showed the lowest activity against breast cancer cells.

Among the amide hybrids of β-carbolines, compounds **13h** with an aminopropanol linker possessed evidently inhibition on the proliferation of breast cancer cells, compared with aminoalcohol linkers, such as **13g**, **13i** and **13j**. As previously noticed, the compounds **13g–j** indicated relatively low IC_{50} values (1.45, 0.89, 1.56 and 1.33 μM, respectively) against MCF-7 cells, compared with the IC_{50} values of **5c**, harmine, positive control doxorubicin (14.3, 16.94, and 3.09 μM, respectively). By contrast, the compounds **13g**, **13h** and **13j** showed the minimum IC_{50} values (0.87, 0.62, and 0.92 μM, respectively) against MDA-MB-231 cells, compared with the IC_{50} values of **5c**, harmine, doxorubicin (12.63, 21.91, and 2.86 μM, respectively). To take these elements into consideration, compound **13h** was the most promising for in depth exploration into the action mechanism against TNBC MDA-MB-231 cells.

Compound **13h** was consisted of the β-carboline moiety (compound **5c**) and furoxan (**9**) through an aminopropanol linker. As shown in Table 1, the IC_{50} values of **13h** against MCF-7 (0.89 μM) and MDA-MB-231 cells (0.62 μM) were obviously lower than that of **5c** (14.3 and 12.63 μM) and **9** (3.92 and 4.84 μM), respectively. These data showed that the potent anti-breast cancer activity of **13h** might be attributed to the synergistic effects of β-carboline and NO donor. Therefore, in order to affirm the contribution of NO to the antiproliferative activity, the NO released concentrations by several selected target derivatives were tested using the Griess assay.[63] As outlined in Fig. 3, hybrids (**13a**, **13d** and **13g–j**) substituted with *p*-methoxyphenyl at position 1 possessed stronger NO release ability than that of analogues substituted with methyl group (**12d**, **12df**, **12h** and **12i**) or H (**11d**, **11e**, **11f** and **11h**). Among compounds **13a**, **13d**, and **13g–j**, the amide hybrids (**13g–j**) released higher NO levels than that of the ester derivatives (**13a** and **13d**). Intriguingly, the most promising compound **13h** produced the highest concentration of NO. These results supported that the NO levels released by several selected target derivatives were positively correlated with their antiproliferative activity against MDA-MB-231 cells.

Numerous compounds suppressed cancer cell growth mainly by decreasing cell division to arrest cell cycle.[64] To verify whether **13h** affects cell cycle progression, propidium iodide (PI) staining-based cell cycle analysis was conducted by flow cytometry. As shown in Fig. 4a, treatment with **13h** hindered the cell cycle at the G2/M stage. Compared to the control cells, the culture of MDA-MB-231 cells with different concentrations of **13h** (0.15, 0.3 and 0.6 μM) enhanced the cells percentage in the G2/M phase from 10.90% to 23.54%, simultaneously the cells percentage of G1 phase reduced, and that of S phase remained essentially unchanged (Fig. 4b). The above results affirmed that **13h** inhibited MDA-MB-231 cells proliferation via arresting cell cycle at G2/M phase.

Since various anticancer drugs cause the tumor cells death through inducing apoptosis,[65] additionally, cell cycle arrest induced by multiple factors may also lead to apoptosis. So whether compound **13h** induced cancerous cell apoptosis was also investigated. Whereafter, vehicle- or **13h**-incubated MDA-MB-231 cells were stained with Annexin V-FITC and PI. As illustrated in Fig. 5a and b, treatment with **13h** caused a concentration-dependent (0.15, 0.3, and 0.6 μM) increase in both the early- and late-stage apoptosis of MDA-MB-231 cells (12.67%, 23.99% and 54.18%, respectively), which demonstrated that **13h** inhibited MDA-MB-231 cells proliferation by inducing apoptosis.

ROS plays a central role in modulating cell apoptosis by disturbing the intracellular environment in various tumor cells, and accesses to the nucleus to inflict DNA damage.[66] Accordingly, to study whether compound **13h** promoted intracellular ROS generation, the 2′,7′-dichlorodihydrofluorescein diacetate (DCFH-DA) was used to survey the levels

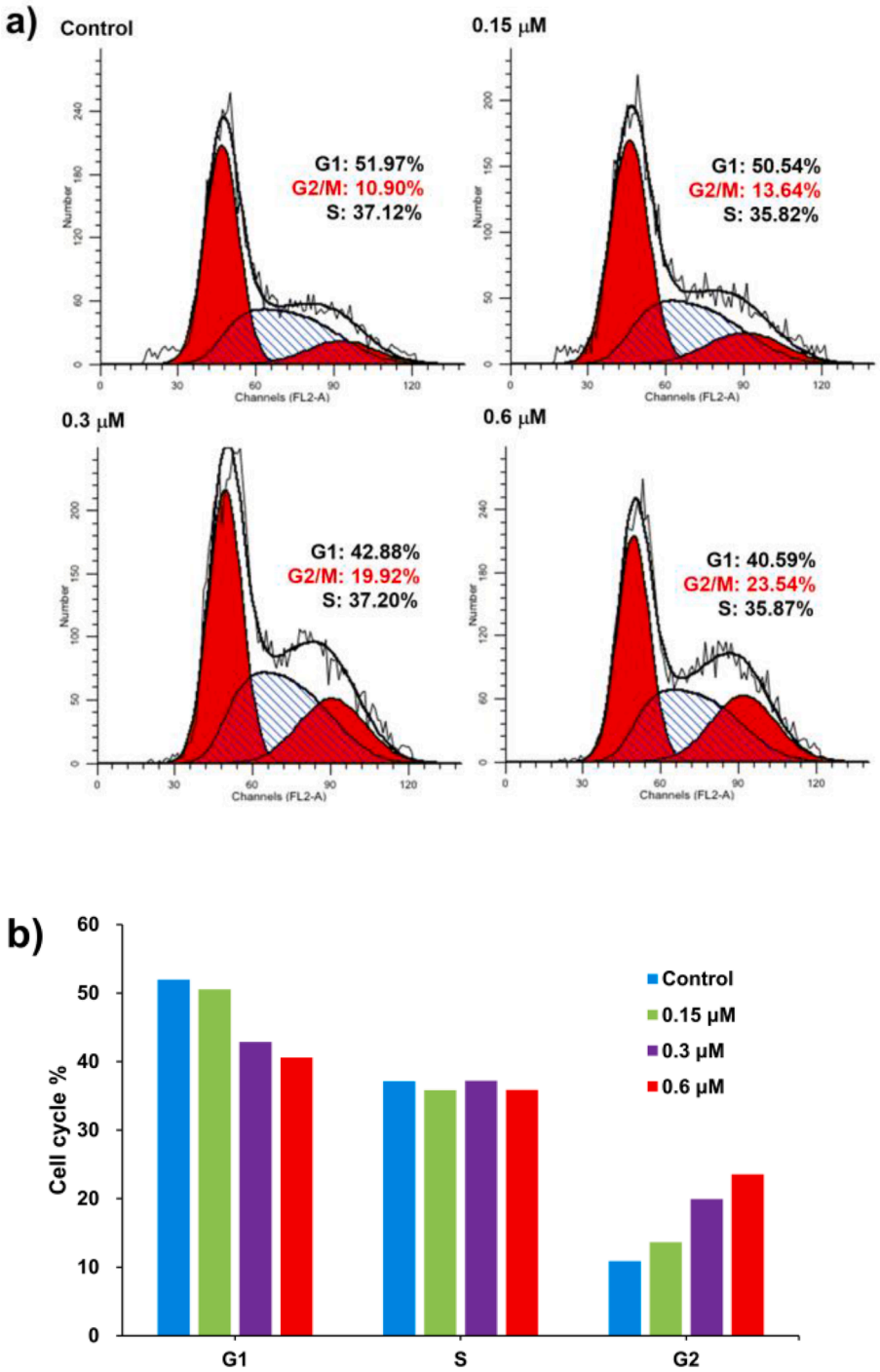

Fig. 4. Compound 13 h induced G2/M arrest in MDA-MB-231 cancer cells. MDA-MB-231 cells were incubated with different concentrations of 13 h (0, 0.15, 0.3, and 0.6 μM) for 72 h. (a) Cells were harvested and stained with PI and then analyzed by flow cytometry. (b) Histograms display the cell cycle distribution percentages.

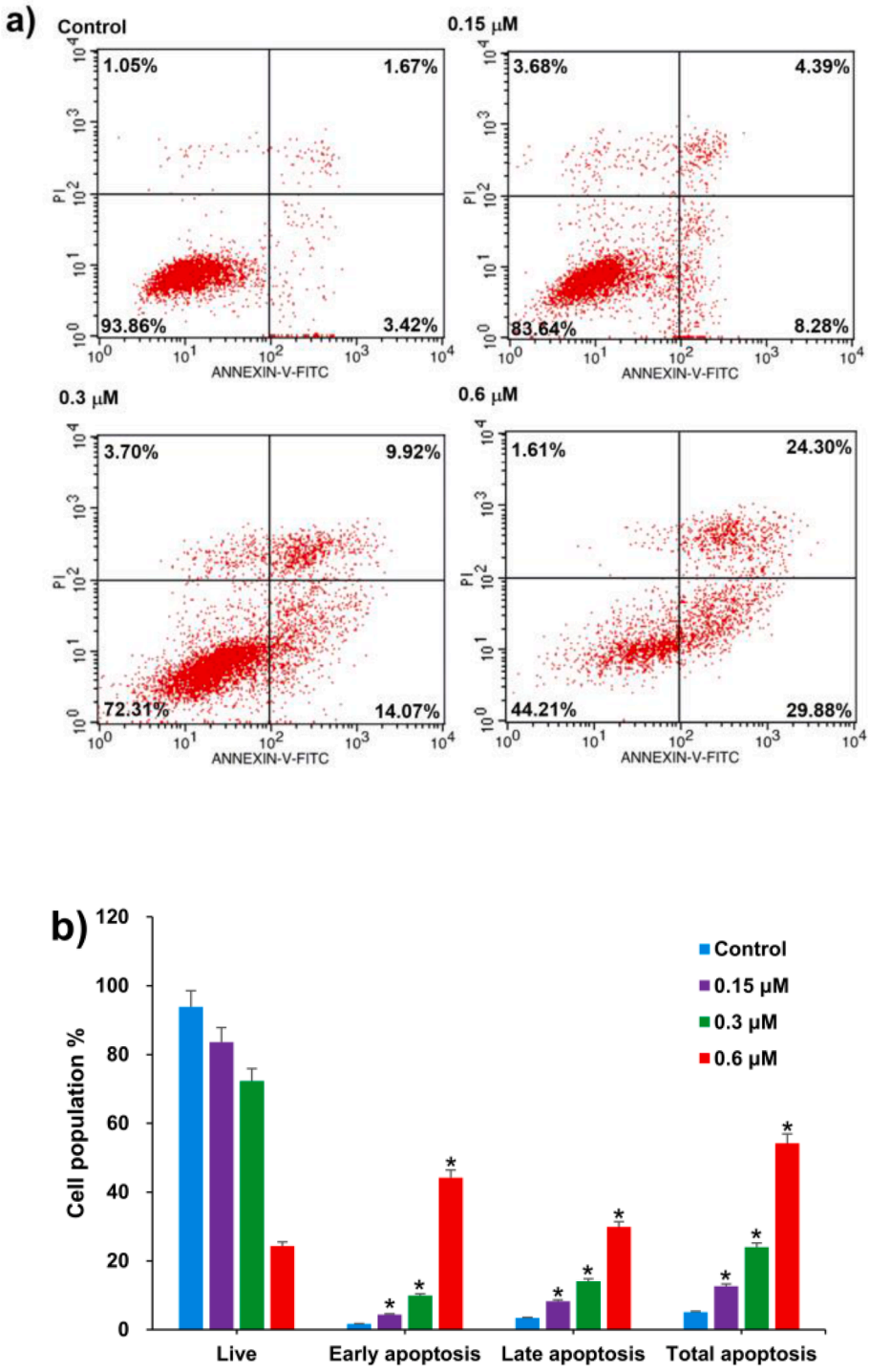

Fig. 5. Compound 13 h induced apoptosis of MDA-MB-231 cells. (a) MDA-MB-231 cells were incubated with varying concentrations of 13 h (0, 0.15, 0.3 and 0.6 μM). After 72 h of incubation, cells were collected and stained with Annexin V/PI, followed by flow cytometric analysis. (b) Histograms display the percentage of cell distribution. Data are represented as mean ± SD of three independent experiments. *$p < 0.05$ vs control group.

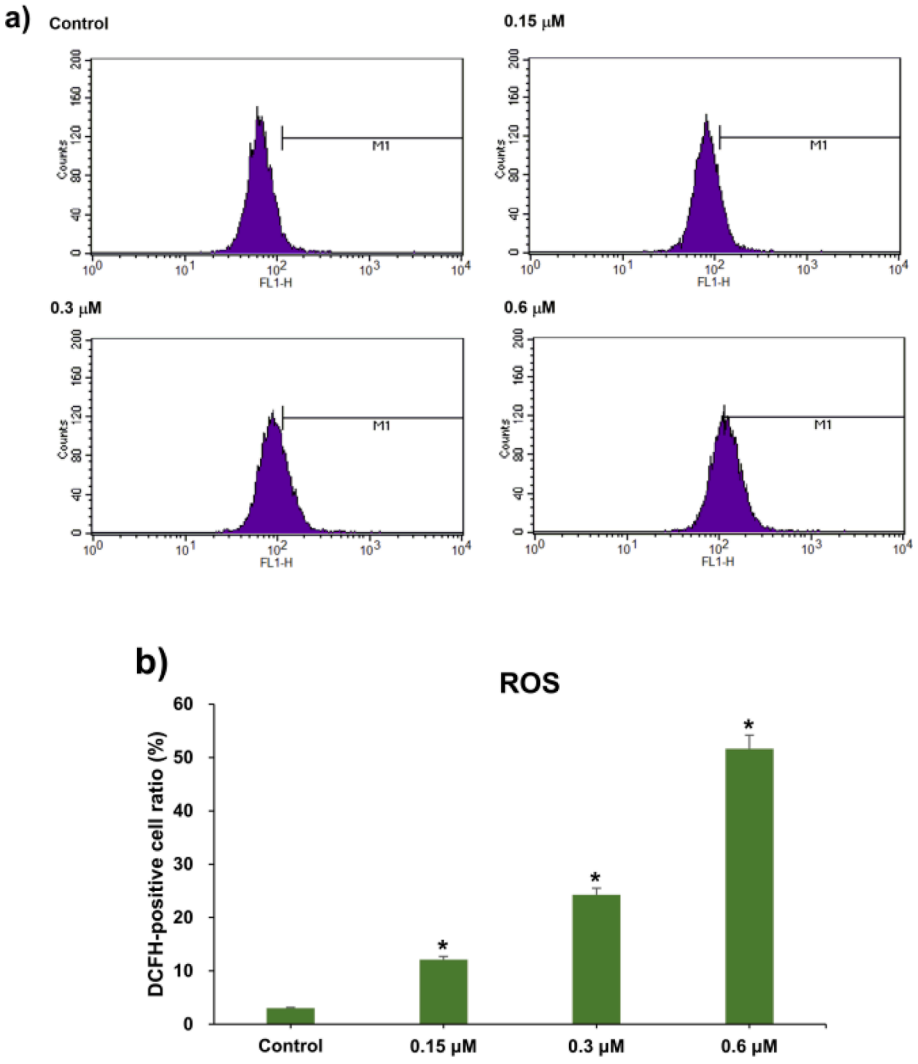

Fig. 6. Accumulation of ROS production in MDA-MB-231 cells induced by 13 h (72 h). (a) Generation of ROS was measured using the ROS-detecting fluorescent dye DCFH-DA in combination with FACScan flow cytometry. (b) Corresponding histograms of FACScan flow cytometry are shown. Data are represented as mean ± SD of three independent experiments. $^{*}p < 0.05$ compared to control cells.

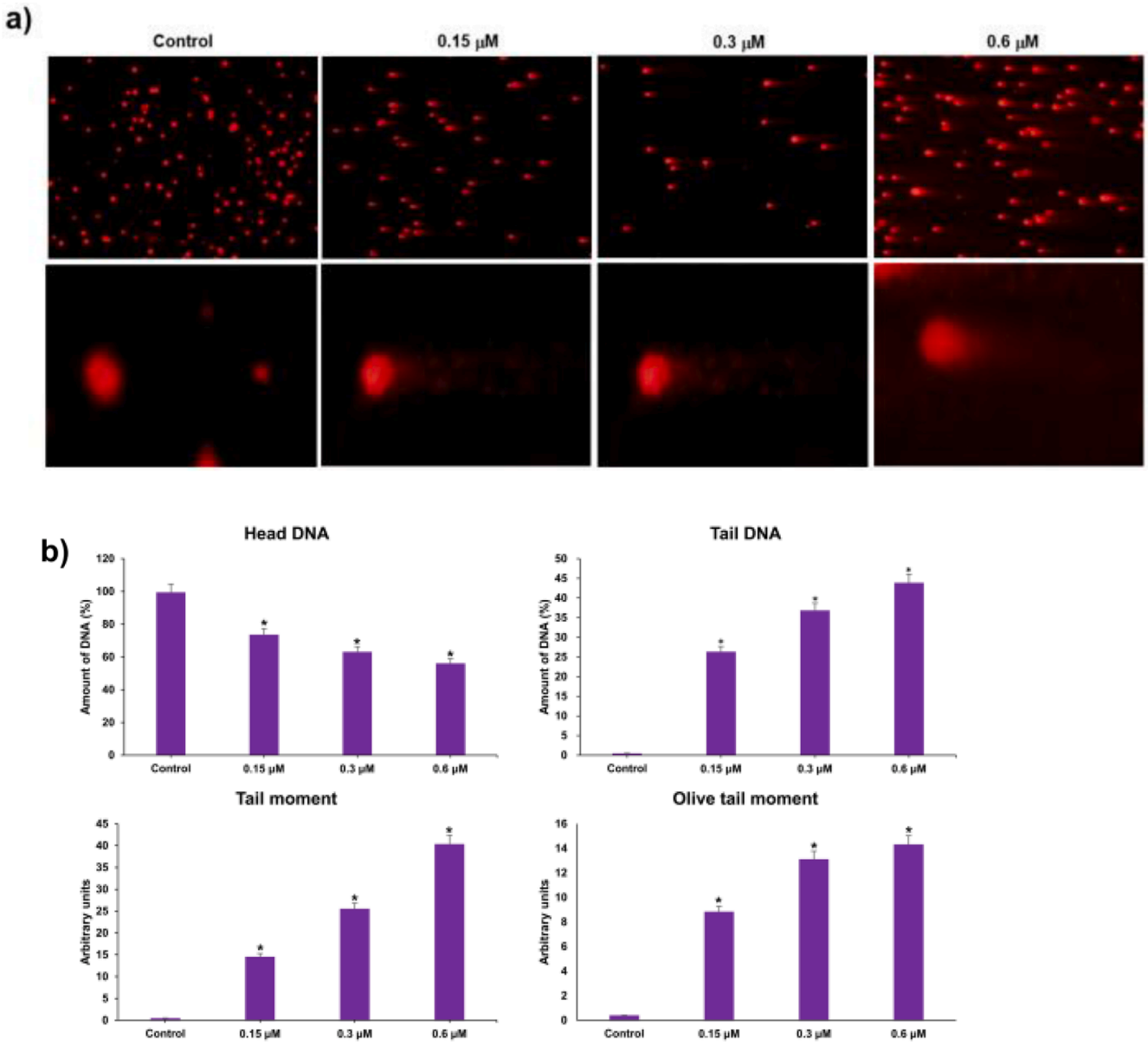

Fig. 7. DNA damage induced by compound 13 h. (a) Cells were incubated for 72 h and DNA damage was evaluated by comet assay. Representative photomicrographs are presented. (b) Head DNA%, tail DNA%, tail movement, and Olive tail movement were measured. Tail and Olive tail movements were presented as estimated DNA damage in arbitrary units. Data are represented as mean ± SD of three independent experiments. $^{*}p < 0.05$ compared to control cells.

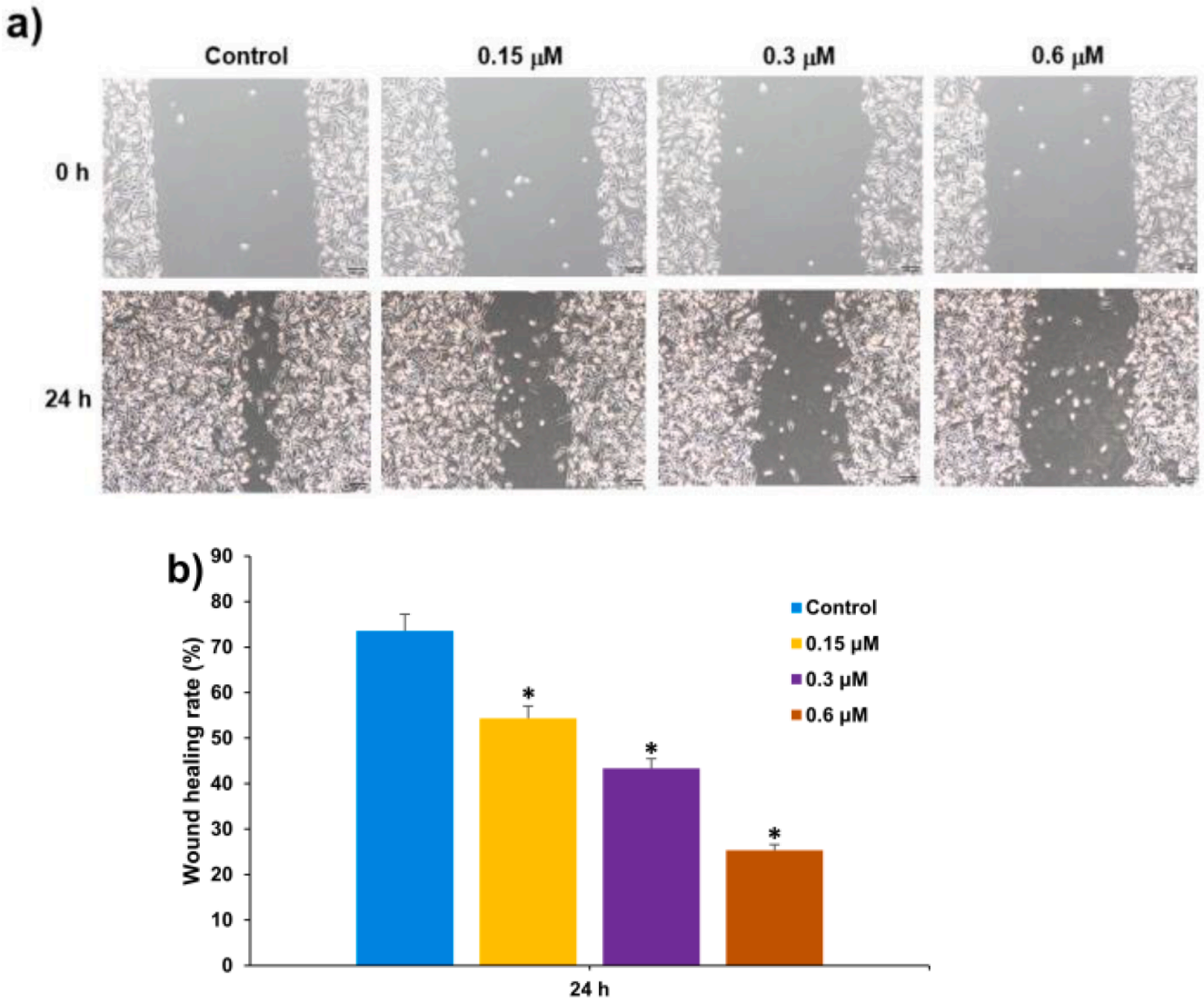

Fig. 8. Effects of 13 h on metastasis, invasion, and adhesion of MDA-MB-231 cells. (a) Scratches of MDA-MB-231 cell colonies were generated with pipette tips (200 μL). After 24 h of incubation with 0, 0.15, 0.3 and 0.6 μM compound 13 h, representative images were captured using phase contrast microscopy. (b) Wound-healing rate of MDA-MB-231 cells induced by 13 h. (c) MDA-MB-231 cells were seeded onto chambers and incubated with 13 h (0, 0.15, 0.3, and 0.6 μM) for 24 h. Cells that migrated through the chambers were stained with crystal violet, and representative images were captured. (d) Histograms display the number of cells. (e) MDA-MB-231 cells were incubated with 13 h (0, 0.15, 0.3 and 0.6 μM) in 96-well plates, and the nonadherent cells were washed away with phosphate-buffered saline, while the adhesive cells were counted using phase contrast microscopy. All data are represented as the mean ± SD of three independent experiments. *$p < 0.05$ vs the control group.

of ROS in the presence and absence of **13h**. As listed in Fig. 6a and 6b, **13h** increased the generation of intracellular ROS in a dose-dependent manner. The DCFH-DA positive cells ratio increased from 3.04% in cells incubated with dimethyl sulfoxide (DMSO) to 51.62% in cells incubated with 0.6 μM **13h**.

As is well known, DNA damage is deemed to a mark of apoptosis. Moreover, it was well documented that excess accumulation of intracellular ROS might led to DNA damage and lipid membrane peroxidation, eventually causing cell death.[67] Therefore, the DNA damage by detecting double-strand DNA breaks (DSBs) adducts in MDA-MB-231 cells using neutral comet assays was evaluated. Fig. 7a revealed that **13h** significantly increased the endogenous DSBs generation. Additionally, **13h** remarkably raised tail DNA percentage with increasing concentration, and by contrast, reduced the head DNA percentage. Meanwhile, DNA migration of tail and Olive tail was perceived with increasing concentration of **13h** (Fig. 7b), announcing that **13h** inhibited DNA replication and induced DNA damage. Taken together, these results preliminarily proved that compound **13h** induced MDA-MB-231 cells apoptosis by stimulating ROS generation, which in turn led to DNA damage.

It is noteworthy that TNBC is the most invasive and metastatic subtype of breast cancer, the effects of compound **13h** on migration and

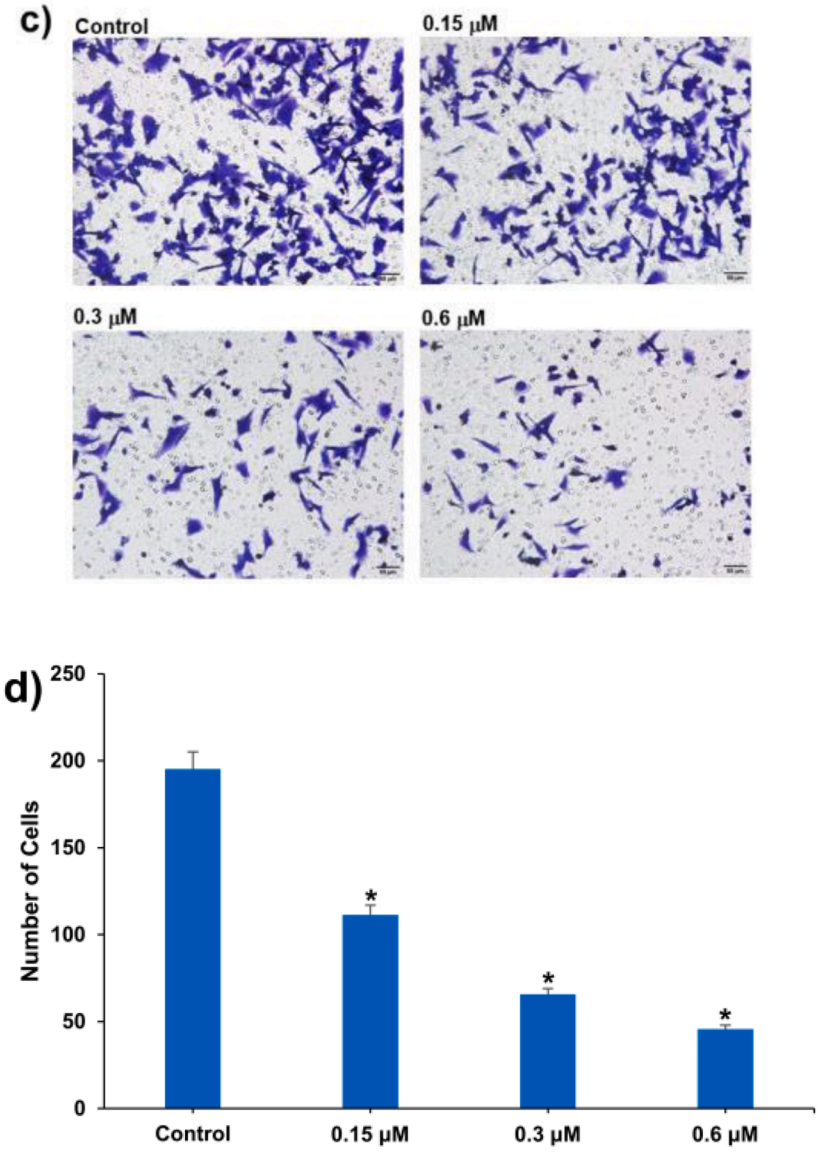

Fig. 8. (*continued*).

invasion by wound healing and transwell assays in MDA-MB-231 cells were further explored. As shown in Fig. 8a and b, after treating without drugs for 24 h, the wound closure distance was significantly shortened, yet the addition of **13h** had remarkable inhibitory effect on wound closure. Moreover, the wound closure rate of cells exposed to 0.3 μM **13h** was less than half compared to the control. With the increasing of **13h** to 0.6 μM, the wound closure rate decreased lower than that treated with 0.3 μM, revealing that **13h** significantly inhibited MDA-MB-231 cells migration via a concentration-dependent manner. The results of the transwell assay are presented in Fig. 8c and d. Treatment with **13h** distinctly restrained the invasion of MDA-MB-231 cells at micromolar concentrations (0.3–0.6 μM). Subsequently, the adhesion assays (Fig. 8**e**) verified that **13h** dose-dependently suppressed the adhesion of MDA-MB-231 cells. As outlined above, **13h** possessed superactive activity against the migration, invasion, and adhesion of MDA-MB-231 cells *in vitro*.

In conclusion, thirty hybrids of *β*-carbolines and (phenylsulfonyl) furoxan (**11a–j**, **12a–j** and **13a–j**) were designed, synthesized and biologically evaluated. After incubating the tumor cells for 72 h, most derivatives presented stronger antiproliferative activity than harmine against MCF-7 and MDA-MB-231 cells. Notably, **13g**, **13h** and **13j** displayed more potent inhibition on MDA-MB-231 cells compared to those of doxorubicin. Particularly, **13h** exhibited the most excellent antiproliferative activity, with an IC_{50} value of 0.62 μM against MDA-MB-231 cells. Interestingly, **13h** also generated a continuous NO release *in vitro*, and produced the NO concentration of above 65 μM/L at 3 h. Accordingly, **13h** was selected for further research to explore the action mechanisms in MDA-MB-231 cell lines. The results demonstrated that **13h** induced G2/M-phase arrest and cell apoptosis by the activation of ROS-mediated DNA damage. Additionally, compound **13h** suppressed the MDA-MB-231 cells metastasis, invasion, and adhesion. Collectively, the novel *β*-carboline-(phenylsulfonyl)furoxan hybrid **13h** possessed prominent antineoplastic activity and sustained NO release capacity *in vitro*. Hence, compound **13h** may be a promising antimetastatic agent for TNBC, which is noteworthy for further investigation.

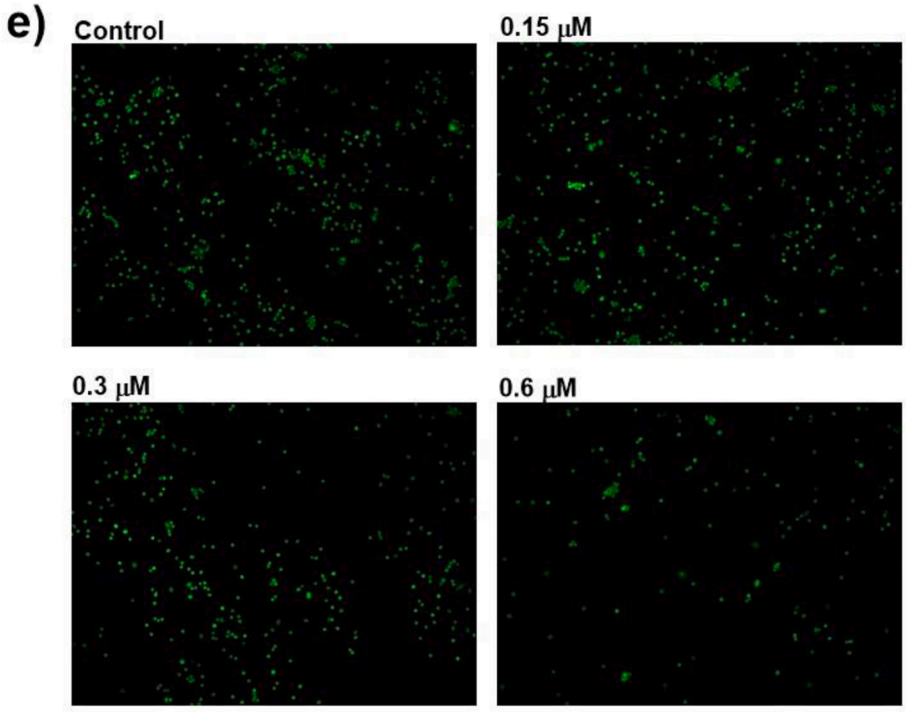

Fig. 8. (*continued*).

Declaration of Competing Interest

The authors declare that they have no known competing financial interests or personal relationships that could have appeared to influence the work reported in this paper.

Acknowledgements

This paper was financially supported by the National Natural Science Foundation of China (81773604) and Career Development Support Plan for Young and Middle-aged Teachers in Shenyang Pharmaceutical University.

Appendix A. Supplementary data

Supplementary data to this article can be found online at https://doi.org/10.1016/j.bmcl.2021.127952.

References

1 Cortes J, Perez-Garcia JM, Llombart-Cussac A, et al. Enhancing global access to cancer medicines. *CA Cancer J Clin*. 2020;70:105–124.
2 Sparano JA, Gray RJ, Makower DF, et al. Adjuvant chemotherapy guided by a 21-gene expression assay in breast cancer. *New Engl J Med*. 2018;379:111–121.
3 DeSantis C, Ma JM, Bryan L, Jemal A. Breast cancer statistics, 2013. *Ca-Cancer J Clin*. 2014;64:52–62.
4 Waks AG, Winer EP. Breast cancer treatment: a review. *JAMA-J Am Med Assoc*. 2019;321:288–300.
5 Brufsky AM, Dickler MN. Estrogen receptor-positive breast cancer: exploiting signaling pathways implicated in endocrine resistance. *Oncologist*. 2018;23:528–539.
6 Carey L, Winer E, Viale G, Cameron D, Gianni L. Triple-negative breast cancer: disease entity or title of convenience? *Nat Rev Clin Oncol*. 2010;7:683–692.
7 Sharma S, Barry M, Gallagher DJ, Kell M, Sacchini V. An overview of triple negative breast cancer for surgical oncologists. *Surg Oncol*. 2015;24:276–283.
8 Costa A, Kieffer Y, Scholer-Dahirel A, et al. Fibroblast heterogeneity and immunosuppressive environment in human breast cancer. *Cancer Cell*. 2018;33:463–479.
9 Audeh MW. Novel treatment strategies in triple-negative breast cancer: specific role of poly(adenosine diphosphate-ribose) polymerase inhibition. *Pharmgenomics Pers Med*. 2014;7:307–316.
10 Miles DW, Diéras V, Cortés J, Duenne AA, Yi J, O'Shaughnessy J. First-line bevacizumab in combination with chemotherapy for HER2-negative metastatic breast cancer: pooled and subgroup analyses of data from 2447 patients. *Ann Oncol*. 2013;24:2773–2780.
11 Islam R, Lam KW. Recent progress in small molecule agents for the targeted therapy of triple-negative breast cancer. *Eur J Med Chem*. 2020;207, 112812.
12 Harvey AL, Edrada-Ebel R, Quinn RJ. The re-emergence of natural products for drug discovery in the genomics era. *Nat Rev Drug Discov*. 2015;14:111–129.
13 Rodrigues T, Reker D, Schneider P, Schneider G. Counting on natural products for drug design. *Nat Chem*. 2016;8:531–541.
14 Newman DJ, Cragg GM. Natural products as sources of new drugs over the nearly four decades from 01/1981 to 09/2019. *J Nat Prod*. 2020;83:770–803.
15 Li SG, Wang YT, Zhang Q, et al. Pegaharmols A-B, axially chiral β-carboline-quinazoline dimers from the roots of *Peganum harmala*. *Org Let*. 2020;22:7522–7525.
16 Ohishi K, Toume K, Arai MA, et al. 9-Hydroxycanthin-6-one, a β-carboline alkaloid from *Eurycoma longifolia*, is the first wnt signal inhibitor through activation of glycogen synthase kinase 3β without depending on casein kinase 1α. *J Nat Prod*. 2015;78:1139–1146.
17 Chen YF, Kuo PC, Chan HH, et al. β-carboline alkaloids from *Stellaria dichotoma* var. lanceolata and their anti-inflammatory activity. *J Nat Prod*. 2010;73:1993–1998.
18 de Oliveira FP, Perdomo RT, Garcez FR, et al. Further constituents of *Galianthe thalictroides* (Rubiaceae) and inhibition of DNA topoisomerases I and IIα by its cytotoxic β-carboline alkaloids. *Bioorg Med Chem Lett*. 2014;24:1358–1361.
19 Le Moigne R, Subra F, Karam M, Auclair C. The β-carboline harmine induces actin dynamic remodeling and abrogates the malignant phenotype in tumorigenic cells. *Cells*. 2020;9:1168.
20 He D, Wu H, Wei Y, et al. Effects of harmine, an acetylcholinesterase inhibitor, on spatial learning and memory of APP/PS1 transgenic mice and scopolamine-induced memory impairment mice. *Eur J Pharmacol*. 2015;768:96–107.
21 Jain S, Panuganti V, Jha S, Roy I. Harmine acts as an indirect inhibitor of intracellular protein aggregation. *ACS Omega*. 2020;5:5620–5628.
22 Farzin D, Mansouri N. Antidepressant-like effect of harmane and other β-carbolines in the mouse forced swim test. *Eur Neuropsychopharmacol*. 2006;16:324–328.
23 Kumar K, Wang P, Wilson J, et al. Synthesis and biological validation of a harmine-based, central nervous system (CNS)-avoidant, selective, human β-cell regenerative dual-specificity tyrosine phosphorylation-regulated kinase A (DYRK1A) inhibitor. *J Med Chem*. 2020;63:2986–3003.
24 Nenaah G. Antibacterial and antifungal activities of (β)-carboline alkaloids of *Peganum harmala* (L) seeds and their combination effects. *Fitoterapia*. 2010;81:779–782.
25 Nguyen HD, Choo YY, Nguyen TD, Nguyen HN, Chau VM, Lee JH. 7-Methoxy-(9H-β-carbolin-1-il)-(E)-1-propenoic acid, a β-carboline alkaloid from *Eurycoma longifolia*, exhibits anti-inflammatory effects by activating the Nrf2/heme oxygenase-1 pathway. *J Cell Biochem*. 2016;117:659–670.
26 Perkovic I, Raic-Malic S, Fontinha D, et al. Harmicines - harmine and cinnamic acid hybrids as novel antiplasmodial hits. *Eur J Med Chem*. 2020;187, 111927.
27 Wu J, Zhao M, Qian K, Lee KH, Morris-Natschke S, Peng S. Novel *N*-(3-carboxyl-9-benzyl-β-carboline-1-yl)ethylamino acids: synthesis, anti-tumor evaluation, intercalating determination, 3D QSAR analysis and docking investigation. *Eur J Med Chem*. 2009;44:4153–4161.

28 Liu Y, He Y, Yang F, et al. A novel synthetic small molecule YF-452 inhibits tumor growth through antiangiogenesis by suppressing VEGF receptor 2 signaling. *Sci China Life Sci*. 2017;60:202–214.
29 Castro AC, Dang LC, Soucy F, et al. Novel IKK inhibitors: β-carbolines. *Bioorg Med Chem Lett*. 2003;13:2419–2422.
30 Funayama Y, Nishio K, Wakabayashi K, et al. Effects of β- and γ-carboline derivatives of DNA topoisomerase activities. *Mutat Res*. 1996;349:183–191.
31 Trujillo JI, Meyers MJ, Anderson DR, et al. Novel tetrahydro-β-carboline-1-carboxylic acids as inhibitors of mitogen activated protein kinase-activated protein kinase 2 (MK-2). *Bioorg Med Chem Lett*. 2007;17:4657–4663.
32 Song Y, Wang J, Teng SF, et al. β-carbolines as specific inhibitors of cyclin-dependent kinases. *Bioorg Med Chem Lett*. 2002;12:1129–1132.
33 Han X, Zhang J, Guo L, et al. A series of β-carboline derivatives inhibit the kinase activity of PLKs. *PLoS ONE*. 2012;7, e46546.
34 Barsanti PA, Wang W, Ni ZJ, et al. The discovery of tetrahydro-β-carbolines as inhibitors of the kinesin Eg5. *Bioorg Med Chem Lett*. 2010;20:157–160.
35 Ling Y, Xu C, Luo L, et al. Novel β-carboline/hydroxamic acid hybrids targeting both histone deacetylase and DNA display high anticancer activity via regulation of the p53 signaling pathway. *J Med Chem*. 2015;58:9214–9227.
36 Ma Y, Wink M. The β-carboline alkaloid harmine inhibits BCRP and can reverse resistance to the anticancer drugs mitoxantrone and camptothecin in breast cancer cells. *Phytother Res*. 2010;24:146–149.
37 Zhao L, Wink M. The β-carboline alkaloid harmine inhibits telomerase activity of MCF-7 cells by down-regulating hTERT mRNA expression accompanied by an accelerated senescent phenotype. *PeerJ*. 2013;1, e174.
38 Ding Y, He J, Huang J, et al. Harmine induces anticancer activity in breast cancer cells via targeting TAZ. *Int J Oncol*. 2019;54:1995–2004.
39 Yamashita N, Kondo M, Zhao S, et al. Picrasidine G decreases viability of MDA-MB 468 EGFR-overexpressing triple-negative breast cancer cells through inhibition of EGFR/STAT3 signaling pathway. *Bioorg Med Chem Lett*. 2017;27:2608–2612.
40 Yeh HT, Tsai YS, Chen MS, et al. Flavopereirine induces cell cycle arrest and apoptosis via the AKT/p38 MAPK/ERK1/2 signaling pathway in human breast cancer cells. *Eur J Pharmacol*. 2019;863, 172658.
41 Szabo C. Gasotransmitters in cancer: from pathophysiology to experimental therapy. *Nat Rev Drug Discov*. 2016;15:185–203.
42 Fukumura D, Kashiwagi S, Jain RK. The role of nitric oxide in tumour progression. *Nat Rev Cancer*. 2006;6:521–534.
43 Bonavida B, Garban H. Nitric oxide-mediated sensitization of resistant tumor cells to apoptosis by chemo-immunotherapeutics. *Redox Biol*. 2015;6:486–494.
44 Chang CF, Diers AR, Hogg N. Cancer cell metabolism and the modulating effects of nitric oxide. *Free Radic Biol Med*. 2015;79:324–336.
45 Bonavida B, Baritaki S, Huerta-Yepez S, Vega MI, Chatterjee D, Yeung KJNO. Novel therapeutic applications of nitric oxide donors in cancer: roles in chemo-and immunosensitization to apoptosis and inhibition of metastases. *Nitric Oxide*. 2008;19:152–157.
46 Pervin S, Singh R, Chaudhuri G. Nitric oxide, N^{ω}-hydroxy-L-arginine and breast cancer. *Nitric Oxide*. 2008;19:103–106.
47 Huang Z, Fu J, Zhang Y. Nitric oxide donor-based cancer therapy: advances and prospects. *J Med Chem*. 2017;60:7617–7635.
48 Lopez-Sanchez LM, Mena R, Guil-Luna S, et al. Nitric oxide-targeted therapy inhibits stemness and increases the efficacy of tamoxifen in estrogen receptor-positive breast cancer cells. Lab Invest 2020; online ahead of print. DOI: 10.1038/s41374-020-00507-z.
49 Martinez L, Thames E, Kim J, Chaudhuri G, Singh R, Pervin S. Increased sensitivity of African American triple negative breast cancer cells to nitric oxide-induced mitochondria-mediated apoptosis. *BMC Cancer*. 2016;16:559.
50 McMurtry V, Saavedra JE, Nieves-Alicea R, Simeone AM, Keefer LK, Tari AM. JS-K, a nitric oxide-releasing prodrug, induces breast cancer cell death while sparing normal mammary epithelial cells. *Int J Oncol*. 2011;38:963–971.
51 Kang F, Zhu J, Wu J, et al. O^2-3-Aminopropyl diazeniumdiolates suppress the progression of highly metastatic triple-negative breast cancer by inhibition of microvesicle formation via nitric oxide-based epigenetic regulation. *Chem Sci*. 2018;9:6893–6898.
52 Gao Y, Sun TY, Bai WF, Bai CG. Design, synthesis and evaluation of novel phenothiazine derivatives as inhibitors of breast cancer stem cells. *Eur J Med Chem*. 2019;183, 111692.
53 Zhao N, Tian KT, Cheng KG, et al. Antiproliferative activity and apoptosis inducing effects of nitric oxide donating derivatives of evodiamine. *Bioorg Med Chem*. 2016;24:2971–2978.
54 Li D, Han T, Tian K, et al. Novel nitric oxide-releasing spirolactone-type diterpenoid derivatives with *in vitro* synergistic anticancer activity as apoptosis inducer. *Bioorg Med Chem Lett*. 2016;26:4191–4196.
55 Jiao R, Xu F, Huang X, et al. Antiproliferative chromone derivatives induce K562 cell death through endogenous and exogenous pathways. *J Enzyme Inhib Med Chem*. 2020;35:759–772.
56 Li D, Hu X, Han T, et al. Synthesis, Biological activity, and apoptotic properties of NO-donor/enmein-type *ent*-kauranoid hybrids. *Int J Mol Sci*. 2016;17:747.
57 Han T, Li J, Xue J, et al. Scutellarin derivatives as apoptosis inducers: Design, synthesis and biological evaluation. *Eur J Med Chem*. 2017;135:270–281.
58 Tian K, Xu F, Gao X, et al. Nitric oxide-releasing derivatives of brefeldin A as potent and highly selective anticancer agents. *Eur J Med Chem*. 2017;136:131–143.
59 Huang X, Cheng K, Liu L, et al. Design, synthesis and apoptosis-related antiproliferative activities of chelidonine derivatives. *Bioorg Med Chem Lett*. 2020;30,126913.
60 Eagon S, Anderson MO. Microwave-assisted synthesis of tetrahydro-β-carbolines and β-carbolines. *European J Org Chem*. 2014;2014:1653–1665.
61 Ling Y, Ye X, Zhang Z, et al. Novel nitric oxide-releasing derivatives of farnesylthiosalicylic acid: synthesis and evaluation of antihepatocellular carcinoma activity. *J Med Chem*. 2011;54:3251–3259.
62 Lakshmi Manasa K, Thatikonda S, Sigalapalli DK, et al. Design and synthesis of β-carboline linked aryl sulfonyl piperazine derivatives: DNA topoisomerase II inhibition with DNA binding and apoptosis inducing ability. *Bioorg Chem*. 2020;101,103983.
63 Kaur J, Bhardwaj A, Huang Z, et al. Synthesis and biological investigations of nitric oxide releasing nateglinide and meglitinide type II antidiabetic prodrugs: *in-vivo* antihyperglycemic activities and blood pressure lowering studies. *J Med Chem*. 2012;55:7883–7891.
64 Strzyz P. Cell signalling: Signalling to cell cycle arrest. *Nat Rev Mol Cell Biol*. 2016;17:536.
65 Evan GI, Vousden KH. Proliferation, cell cycle and apoptosis in cancer. *Nature*. 2001;411:342–348.
66 Zheng A, Li H, Wang X, et al. Anticancer effect of a curcumin derivative B63: ROS production and mitochondrial dysfunction. *Curr Cancer Drug Targets*. 2014;14:156–166.
67 Wu CF, Efferth T. Miltirone induces G2/M cell cycle arrest and apoptosis in CCRF-CEM acute lymphoblastic leukemia cells. *J Nat Prod*. 2015;78:1339–1347.